Egypt. J. Chem. **Vol. 68,** SI: Z. M. Nofal, pp. 105 - 119 (2025)

Egyptian Journal of Chemistry

http://ejchem.journals.ekb.eg/

Fraction Derived from *Lansium domesticum* Leaves Triggers Cell Cycle Arrest and Apoptosis in 4T1 Cell Line Via Cdk-2 and p-53 Proteins Modulation

Ana Yulyana [1], Poppy Anjelisa Zaitun Hasibuan [2], Sumaiyah Sumaiyah [3], Kasta Gurning [4], Ririn Astyka [5], Akramul Khair Annava [5], Muhammad Fauzan Lubis [5]*

[1]*Department of Pharmacy, Faculty of Pharmacy, Institut Sains dan Teknologi Nasional, Medan, Indonesia*

[2]*Department of Pharmacology, Faculty of Pharmacy, Universitas Sumatera Utara, Medan, Indonesia*

[3]*Department of Pharmaceutical Technology, Faculty of Pharmacy, Universitas Sumatera Utara, Medan, Indonesia*

[4]*Department of Pharmacy, Faculty of Pharmacy, Institut Kesehatan Senior Medan, Medan, Indonesia*

[5]*Department of Pharmaceutical Biology, Faculty of Pharmacy, Universitas Sumatera Utara, Medan, Indonesia*

Abstract

This study investigates the anticancer potential of ethanolic extracts (EEL) and fractions derived from *Lansiumdomesticum* leaves, with a particular focus on the fourth fraction of EEL (EELD), against the murine 4T1 breast cancer cell line. EELD demonstrated significant cytotoxic activity, with an IC_{50} of 72.75 ± 2.98 µg/mL and a selectivity index (SI) of 4.69, indicating notable selectivity toward cancer cells compared to normal cells. Flow cytometry analysis revealed that EELD induced cell cycle arrest at the Sub G1 phase and promoted apoptosis in a dose-dependent manner. Immunocytochemical evaluation showed upregulation of p53 and suppression of Cdk-2 expression, highlighting the involvement of intrinsic apoptotic pathways.Phytochemical analysis identified bioactive compounds, including hexadecanoic acid, methyl ester, and trans-13-octadecenoic acid, methyl ester, which are associated with anticancer and antioxidant properties. These findings suggest that EELD's anticancer activity is mediated through a combination of cell cycle regulation, apoptosis induction, and bioactive compound synergy. While EELD exhibits promising anticancer properties, its efficacy remains lower than the standard chemotherapeutic agent doxorubicin. Further, in vivo studies and molecular investigations are required to optimize its therapeutic potential and elucidate its mechanisms of action. This study highlights the potential of *L. domesticum* as a source of plant-derived anticancer agents and provides a foundation for future research into its therapeutic applications.

Keywords: *Lansiumdomesticum* leaf; Fractionations; 4T1 breast cancer cells; cell cycle arrest; apoptosis; bioactive compounds

1. Introduction

Cancer remains a significant global health burden, driving the demand for innovative therapeutic strategies [1]. Natural products have long served as a rich source of bioactive compounds, with plant-based therapies demonstrating considerable potential in combating various types of cancer [2], [3], [4]. Among such plants, *Lansiumdomesticum* has garnered attention for its diverse pharmacological properties, including antioxidant [5], anti-inflammatory [6], and anticancer effects [7].

Extracts from various parts of *L. domesticum*, including fruits, leaves, and bark, have shown cytotoxic effects against several cancer cell lines, particularly colorectal [8] and lung cancer [9]. These anticancer activities have been attributed to the presence of bioactive compounds such as terpenoids, flavonoids, and alkaloids [10], [11]. The mechanisms of action reported in these studies include induction of cell cycle arrest, promotion of apoptosis, and modulation of key signaling pathways, such as the PI3K/Akt pathway [12].

While these findings highlight the therapeutic potential of *L. domesticum*, most studies have focused on crude extracts, which often comprise a complex mixture of compounds. This complexity can mask or dilute the

*Corresponding author e-mail: fauzan.lubis@usu.ac.id.; (**Muhammad Fauzan Lubis**).
Received date 13 January 2025; Revised date 05 May 2025; Accepted date 18 May 2025
DOI: 10.21608/EJCHEM.2025.352613.11159

activity of individual bioactive components, necessitating further fractionation and isolation of active subfractions. By isolating sub-fractions, researchers can identify specific compounds responsible for the observed bioactivity and gain deeper insights into their molecular mechanisms of action. As reported by Mayanti et al. (2025), Onoceranoidtriterpenes obtained from the ethyl acetate fraction of *L. domesticum* fruit peel exhibited strong cytotoxic effects against MCF-7 breast cancer cells [13]. In addition, a sesquiterpene aldehyde isolate from the ethyl acetate fraction of *L. domesticum* fruit peel also demonstrated strong cytotoxic activity against T47D breast cancer cells and HepG2 liver cancer cells [14]. Nevertheless, fractionation serves as an initial step in discovering isolates that can be further developed as novel anticancer agents.

Building on this foundation, the current study aims to investigate the anticancer potential of a fraction derived from *L. domesticum* leaves. Specifically, this study evaluates its ability to induce cell cycle arrest and apoptosis in the 4T1 cell line, a murine model of triple-negative breast cancer known for its aggressive and metastatic characteristics. This research seeks to extend the understanding of *L. domesticum's* therapeutic potential and contribute to the development of more targeted plant-derived anticancer agents.

2. Materials and Methods

2.1. Plant material and extraction

The leaves of *L. domesticum* were collected from Delitua, Deli Serdang, North Sumatera, Indonesia, during May 2024. The plant material was identified and authenticated by Prof. Dr. Etti Sartina Siregar, a botanist from Universitas Sumatera Utara, Indonesia, based on morphological and taxonomical characteristics. A voucher specimen (Voucher No. 2875/MEDA/2024) was deposited at the Herbarium Medanese (MEDA) of Universitas Sumatera Utara, Indonesia, for future reference.

Upon collection, the leaves were thoroughly washed with distilled water to remove dirt and impurities. The cleaned leaves were then air-dried in a shaded, well-ventilated area at room temperature for 3 days until they reached a constant weight. After drying, the leaves were ground into a fine powder using a mechanical grinder and sieved to ensure uniform particle size. The resultant dry leaf powder was stored in an airtight container to prevent moisture absorption and contamination. The container was kept in a cool, dark place at 2-8°C to maintain the stability and integrity of the plant material until further processing.

The dry leaf powder was subjected to extraction using absolute ethanol as the solvent (Sigma-Aldrich, USA). The extraction was carried out using the reflux method, where 100 g of the leaf powder was mixed with 1 L of absolute ethanol. The mixture was refluxed at 70–80°C for 2 hours to ensure efficient extraction of bioactive compounds. After completion, the extract was filtered through Whatman No. 1 filter paper to remove plant debris. The filtrate was then concentrated under reduced pressure using a rotary evaporator at 40°C to obtain a crude ethanol extract. The crude extract was stored in a sealed amber vial at 2-8°C until further fractionation and analysis [15].

2.2. Fractionation of extract

The 3 g of crude ethanol extract of *L. domesticum* leaves (EEL) was subjected to silica vacuum column chromatography (Silica gel 60, 230-400 Mesh ASTM, Merck, Germany) followed by gradient elution of n-hexane: ethyl acetate (Sigma-Aldrich, USA). All fractions were analyzed using thin-layer chromatography (TLC) with the reagent spotted with 50% sulfuric acid (Sigma-Aldrich, USA). Then, fractions with the same TLC profile were combined. Eventually, five fractions were obtained for further testing (Table 1) [16].

2.3. Cytotoxic activity and selectivity assay

The cytotoxicity and selectivity of the EEL and its five subfractions (EELA (first fraction), EELB (second fraction), EELC (third fraction), EELD (fourth fraction), and EELE (fifth fraction)) were evaluated using the MTT assay (Sigma-Aldrich, USA) on the 4T1 cell line. The MTT assay assesses cell viability by measuring the reduction of MTT [3-(4,5-dimethyl thiazol-2-yl)-2,5-diphenyltetrazolium bromide] into formazan crystals by mitochondrial dehydrogenases in metabolically active cells.

2.3.1. Cell culture

The 4T1 cells were cultured in RPMI-1640 (Sigma-Aldrich, USA) supplemented with 10% fetal bovine serum (FBS) (Sigma-Aldrich, USA) and 1% penicillin-streptomycin (Sigma-Aldrich, USA), and maintained at 37°C in a humidified incubator with 5% CO_2. The cells were seeded in a 96-well plate at a density of 5×10^3 cells/well and incubated for 24 hours to allow for cell attachment.

Table (1): Result of fractionation from the ethanolic extract *Lansium domesticum* leaf

Final fraction	Weight (g)	Yield (%)	Rf
EELA	0.021	0.7	0.8375 (blue)
			0.8875 (blue)
EELB	0.120	4.00	0.725 (red)
			0.8125 (red)
			0.875 (red)
EELC	0.489	16.3	0.3125 (red)
			0.4375 (red)
			0.5625 (red)
			0.6875 (purple)
			0.8125 (red)
			0.875 (blue)
EELD	0.610	20.33	0.125 (blue)
			0.3125 (red)
			0.4375 (red)
			0.5625 (red)
			0.6875 (purple)
			0.8125 (red)
			0.875 (blue)
EELE	0.350	11.66	0.125 (blue)
			0.3125 (red)
			0.4375 (red)
			0.5625 (red)
			0.6875 (purple)
			0.8125 (red)
			0.875 (blue)

2.3.2. MTT assay

The EEL and fractions were dissolved in dimethyl sulfoxide (DMSO, Merck, Germany) to prepare stock solutions and further diluted with complete medium to final concentrations ranging from 31.25 µg/mL to 500 µg/mL. A negative control (medium only) and a positive control (doxorubicin) were included in each experiment. After 24 hours of seeding, the medium in each well was replaced with 100 µL of the EEL or fractions solution at the desired concentrations. Therefore, following the treatment period, 10 µL of MTT solution (5 mg/mL in Phosphate-buffered saline (PBS)) was added to each well and incubated at 37°C for 4 hours. After incubation, the medium containing MTT was carefully removed, and 100 µL of DMSO was added to each well to dissolve the formazan crystals. The plate was shaken gently for 10 minutes to ensure complete solubilization. Absorbance was measured at 570 nm using a microplate reader. Cell viability (%) was calculated using Equation 1 [17]:

$$Cell\ viability\ (\%) = \frac{Abs\ of\ treated\ cell}{Abs\ of\ control\ cell}\ x\ 100\%\ (1)$$

Meanwhile, the half-maximal inhibitory concentration (IC_{50}) was determined by plotting a dose-response curve using the cell viability data and performing nonlinear regression analysis. IC_{50} values were calculated for the EEL and each fraction. On the other hand, to evaluate the selectivity of the EEL and fractions, a selectivity index (SI) was calculated using Equation 2 [18]:

$$SI = \frac{IC50\ on\ vero\ cells}{IC50\ on\ 4T1\ cells}\ (2)$$

An SI > 2 was considered indicative of selective cytotoxicity towards cancer cells.

2.4. Cell cycle inhibition assay by flow cytometry

Seed 4T1 cells in 6-well plates at a density of 2×10^5 cells/well and incubate cells for 24 hours at 37°C in a humidified incubator with 5% CO_2 to allow for attachment. Treat cells with the selected fraction at concentrations of 1/2 IC_{50} and 1/5 IC_{50}. Then, the treated cells were incubated for 24 hours. After treatment, detach the cells using trypsin-EDTA (Merck, Germany) and collect both adherent and floating cells. Wash the cells twice with cold PBS (centrifuge at 300 × g for 5 minutes between washes). Resuspend the cell pellet in 1 mL of cold PBS. Fix the cells by slowly adding 2 mL of chilled 70% ethanol while vortexing gently to prevent clumping. Incubate the cells at -20°C for 2 hours. Afterward, wash the fixed cells twice with PBS to remove

ethanol. Resuspend the cell pellet in 500 µL of PBS containing RNase A (50 µg/mL, Merck, Germany) and propidium iodide (50 µg/mL, Merck, Germany). Incubate the cells in the dark at 37°C for 30 minutes. Eventually, the stained cells will be analyzed using a flow cytometer [19].

2.5. Apoptosis analysis by flow cytometry

The apoptosis-inducing effect of the most active fraction of EEL was evaluated using flow cytometry with Annexin V-FITC (Merck, Germany) and propidium iodide (PI, Merck, Germany) staining. 4T1 cells were seeded in 6-well plates at a density of 2×10^5 cells/well and incubated for 24 hours in a humidified incubator at 37°C with 5% CO_2 to allow for attachment. Cells were treated with the fraction at concentrations of 1/2 IC_{50} and 1/5 IC_{50}, along with untreated controls. Following 24 hours of treatment, both adherent and floating cells were collected by trypsinization and centrifuged at 300 × g for 5 minutes. Afterwards, the cell pellets were washed twice with cold PBS and resuspended in 100 µL of 1× binding buffer (provided with the Annexin V-FITC Apoptosis Detection Kit). Subsequently, 5 µL of Annexin V-FITC and 5 µL of PI solution (50 µg/mL) were added to the suspension, followed by gentle mixing. The cells were incubated in the dark at room temperature for 15 minutes to ensure effective staining. After incubation, an additional 400 µL of 1× binding buffer was added to each sample, and the cells were immediately analyzed using a flow cytometer equipped with a 488 nm laser for excitation. At least 10,000 events per sample were collected, and the data were analyzed using appropriate flow cytometry software to differentiate between live, early apoptotic, late apoptotic, and necrotic cells based on Annexin V-FITC and PI fluorescence intensities [20].

2.6. Cdk-2 and p53 analysis using immunocytochemistry

This study was conducted according to a previous test by Fitri et al. (2023) with slight modifications [21]. Briefly, 4T1 cells were seeded on sterile glass coverslips placed in 6-well plates at a density of 2×10^5 cells/well. The cells were incubated at 37°C in a humidified incubator with 5% CO_2 for 24 hours to allow for attachment. Subsequently, the cells were treated with the fraction at concentrations of 1/2 IC_{50} and 1/5 IC_{50}, along with untreated for 24 hours.

After treatment, the medium was removed, and the cells were washed twice with PBS to remove the residual medium. The cells were then fixed with 4% paraformaldehyde for 15 minutes at room temperature, followed by permeabilization with 0.1% Triton X-100 in PBS for 10 minutes. After permeabilization, the cells were washed and incubated with a blocking solution (5% bovine serum albumin in PBS) for 30 minutes at room temperature to reduce non-specific antibody binding.

Subsequently, the cells were incubated with primary antibodies specific to Cdk-2 and p53 (anti-Cdk 2 and anti-p53 monoclonal antibodies) diluted in a blocking solution according to the manufacturer's recommendations. The incubation was carried out overnight at 4°C in a humidified chamber to ensure specific binding of the antibodies to their respective targets. After primary antibody incubation, the cells were washed three times with PBS to remove unbound antibodies.

Moreover, the cells were then incubated with secondary antibodies conjugated to fluorophores (Alexa Fluor 488) for 1 hour at room temperature in the dark. Following secondary antibody incubation, the cells were washed three times with PBS. The cells were incubated with DAPI (4′,6-diamidino-2-phenylindole) for 5 minutes to counterstain the nuclei, then washed with PBS.

Ultimately, the coverslips were mounted onto glass slides using an anti-fade mounting medium and sealed with clear nail polish. The slides were visualized using a fluorescence microscope, and images were captured at appropriate magnifications. Cdk-2 and p53 expression levels were assessed by analyzing the fluorescence intensity of the specific staining in treated and control groups. Quantification of fluorescence intensity was performed using image analysis software (ImageJ), and the results were statistically compared to evaluate the effect of the fraction on Cdk-2 and p53 expression.

2.7. Phytochemical analysis of active fraction

The chemical composition of the most active fraction of EEL was analyzed using gas chromatography-mass spectrometry (GC-MS). For GC-MS analysis, the fraction was dissolved in high-purity methanol at a concentration of 1 mg/mL, and the solution was filtered through a 0.22 µm syringe filter to remove particulates. The analysis was performed on a TRACE 1310 GC coupled with an ISQ LT Single Quadrupole Mass Spectrometer from Thermo ScientificTM and equipped with an HP-5MS capillary column (30 m × 0.25 mm, 0.25 µm film thickness). Helium was used as the carrier gas at a constant flow rate of 1 mL/min. The injector temperature was set at 230°C, and the sample (1 µL) was injected in split mode with a split ratio of 1:50. The oven temperature program was set to start at 50°C, held for 2 minutes, and then increased to 325°C at a rate of 10°C/min, with a final hold time of 8 minutes. Mass spectra were acquired in electron ionization (EI) mode at 70 eV over a mass range of 40–500 m/z. Peaks were identified by comparing the mass spectra with entries in the NIST Mass Spectral Library.

2.8. Statistical analysis

All experiments were conducted in triplicate, and data were presented as mean ± standard deviation (SD). Statistical analyses were performed using GraphPad Prism version 9.0. The differences between groups were analyzed using a one-way analysis of variance (ANOVA) followed by Tukey's test to compare multiple groups. For comparisons between the two groups, an independent sample t-test was employed. The level of statistical significance was set at $p<0.05$. Eventually, statistical analysis and graphical representation of data were performed to ensure clarity and reproducibility.

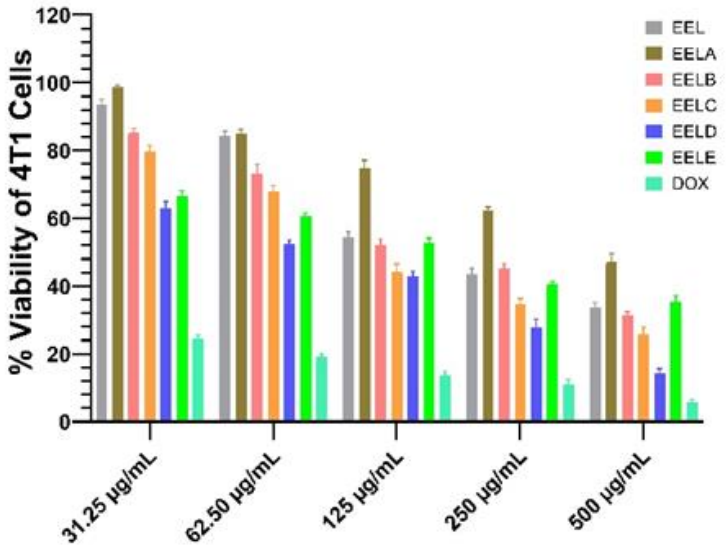

Figure (1): % Viability of 4T1 cells after administration of EEL and its fractions

3. Results

3.1. Yield of fraction

The fractionation process was carried out on EEL using vacuum liquid chromatography with a mobile phase that was determined according to what was stated in the test procedure. Then the fractionation results can be seen in Table 1. The chromatogram obtained was detected with a 50% sulfuric acid under UV 366 nm. The chromatogram of each fraction was calculated for its Rf value so that fractions that had chromatograms with similar Retention factor (Rf) would be combined. From the results of the combination, 5 fractions were obtained, namely EELA (0.021 g), EELB (0.120 g), EELC (0.489 g), EELD (0.610 g), and EELE (0.350 g), which would then be used in further tests.

Table (2): The Inhibitory Concentration 50 (µg/mL) and selectivity index of each sample

Sample	IC_{50} (µg/mL)		SI
	4T1 cells	Vero cells	
EEL	159.8 ± 3.86[a]	456.87 ± 3.67[a]	2.85[a]
EELA	427.86 ± 5.79[b]	689.32 ± 2.56[b]	1.61[b]
EELB	169.45 ± 3.90[c]	424.98 ± 4.12[c]	2.50[c]
EELC	112.33 ± 3.24[d]	374.65 ± 5.32[d]	3.33[d]
EELD	72.75 ± 2.98[e]	341.54 ± 4.87[e]	4.69[e]
EELE	152.12 ± 4.65[f]	378.18 ± 4.50[f]	2.48[f]
DOX	12.64 ± 1.64[g]	146.23 ± 3.71[g]	11.55[g]

Different letters in each result presented that the data is significantly different from other samples ($p<0.05$).

3.2. Cytotoxic activity of extract and fractions

Cytotoxic activity testing of EEL and fractions was conducted using an MTT assay against 4T1 cells. The purpose of this test was to determine whether the samples of EEL and fractions had a cytotoxic effect on 4T1 cells. The % viability of 4T1 cells after administration of EEL and fractions is presented in Figure 1.

Figure 1 demonstrates the cytotoxic activity of the EEL and its fractions (EELA, EELB, EELC, EELD, and EELE) against murine breast cancer cells 4T1, with Doxorubicin (DOX) as a positive control. The results showed that cell viability consistently decreased with increasing concentrations for all tested samples ($p<0.0001$), indicating a significant dose-response relationship.At the lowest concentration (31.25 µg/mL), EELA exhibited the highest viability, reflecting low cytotoxic activity with an average cell viability of 98.63 ± 0.67%, followed by EEL (93.58 ± 1.53%) and EELB (85.31 ± 1.12%). In contrast, DOX, as a positive control, showed significantly lower cell viability at the same concentration (24.52 ± 1.03%), indicating its much stronger cytotoxic potential compared to the extract and fractions.At intermediate concentrations (125 µg/mL), EEL and its fractions showed a significant reduction in cell viability. EEL exhibited a viability of 54.50 ± 1.60%, while EELA and EELE showed higher viability values, at 74.90 ± 2.19% and 52.81 ± 1.25%, respectively. Other fractions, such as EELC (44.26 ± 2.28%) and EELD (42.99 ± 1.48%), demonstrated higher cytotoxic potential compared to EELA.Overall, these data suggest that the cytotoxic activity of the extract and its fractions against 4T1 cells varies significantly depending on the concentration used. Fractions EELD and EELC showed better activity than the other fractions, although their potency was still lower than DOX as a standard cytotoxic agent.

The present study evaluated the cytotoxic activity and selectivity of an EEL and its fractions (EELA, EELB, EELC, EELD, and EELE) against 4T1 murine breast cancer cells and Vero normal cells, with DOX serving as the positive control. The IC_{50} values and Selectivity Index (SI) were calculated, and statistical analysis ($p<0.05$) revealed significant differences among the tested samples, as denoted by distinct superscript letters (Table 2).DOX exhibited the highest cytotoxic activity with an IC_{50} of 12.64 ± 1.64 µg/mL in 4T1 cells and the lowest IC_{50} in Vero cells (146.23 ± 3.71 µg/mL), resulting in the highest SI of 11.55. This underscores DOX's superior potency and selectivity. Among the sample tests, EELD emerged as the most promising candidate, demonstrating the lowest IC_{50} (72.75 ± 2.98 µg/mL) in 4T1 cells and a relatively low IC_{50} (341.54 ± 4.87 µg/mL) in Vero cells, yielding the highest SI (4.69) among the sample tests. These findings indicate that EELD has a notable therapeutic window, making it a potential candidate for further anticancer studies. EELC also showed favorable activity with an IC_{50} of 112.33 ± 3.24 µg/mL and an SI of 3.33, indicating moderate selectivity.Other fractions, including EEL, EELB, and EELE, displayed intermediate cytotoxic activities with IC_{50} values ranging from 152.12 ± 4.65 µg/mL to 169.45 ± 3.90 µg/mL in 4T1 cells and SI values between 2.48 and 2.85. In contrast, EELA exhibited the weakest cytotoxicity with an IC_{50} of 427.86 ± 5.79 µg/mL in 4T1 cells and the lowest SI of 1.61, indicating poor selectivity and limited therapeutic potential. The significant differences in IC_{50} and SI among the samples reflect the diverse cytotoxic profiles and selectivity of these extracts and fractions.Overall, EELD demonstrates the most promising anticancer potential among the extracts due to its potent cytotoxicity and high selectivity. However, its efficacy is still lower than DOX, highlighting the need for further research to optimize its bioactivity and elucidate its mechanism of action. These findings support the exploration of EELD and EELC as potential anticancer agents in preclinical and clinical studies.

3.3. Cell cycle arrest activity of EELD

Related to the IC_{50} and SI values of each sample, the EELD was nominated for further testing, including the observation of cell cycle arrest activity. The effect of EELD on inhibiting the cell cycle of 4T1 was conducted at 1/2 IC_{50} and 1/5 IC_{50} of EELD. Cell cycle arrest of 4T1 cells after administration of EELD is presented in Figure 2.

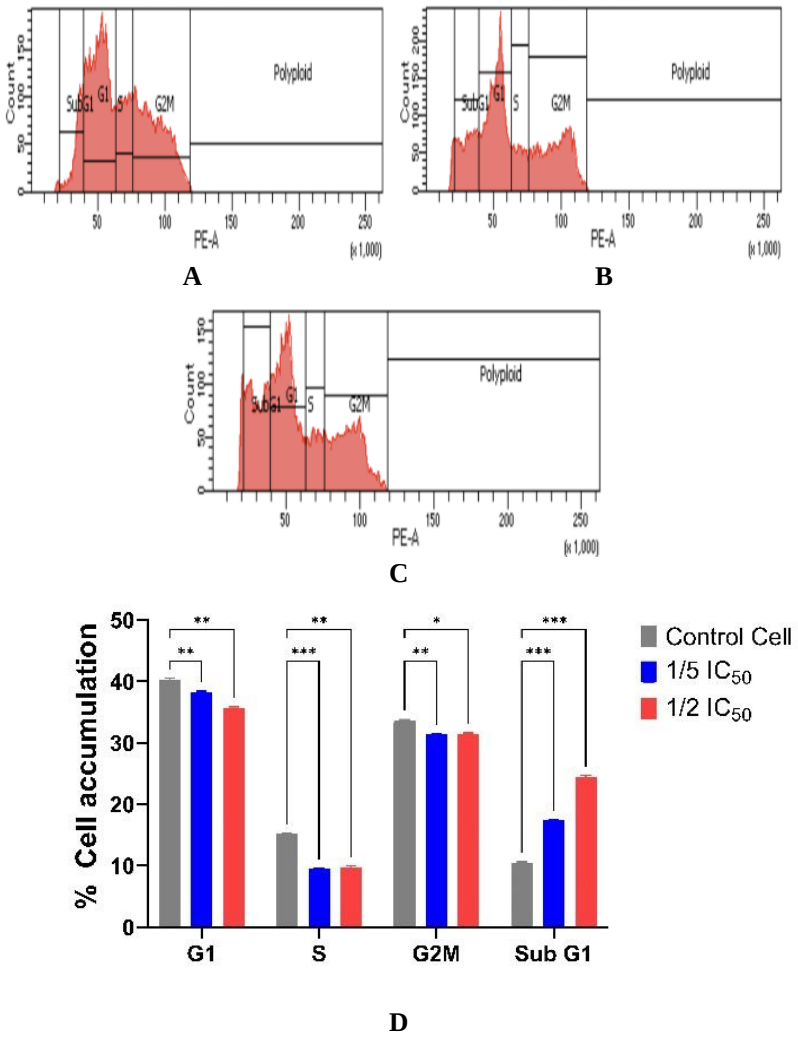

Figure (2): % Cell accumulation of 4T1 cells after administration of 1/5 and 1/2 IC_{50} of EELD. (A) The distribution of 4T1 cells in the control cell group, (B) 4T1 cells in 1/5 IC_{50} of the EELD group, and (C) 4T1 cells in 1/2 IC_{50} of the EELD group. (D) % Cell accumulation in each phase. *Indicated that value is significantly different with $p<0.05$, **Indicated that value is significantly different with $p<0.01$, and ***Indicated that value is significantly different with $p<0.001$.

The study investigated the impact of EELD on the cell cycle distribution of 4T1 cells, analyzing cell accumulation percentages in the control group and after administration of EELD at 1/5 and 1/2 of its IC_{50} concentration. Statistical significance was assessed, with p-values denoted as *$p<0.05$, **$p<0.01$, and ***$p<0.001$.The control group exhibited a baseline distribution of cells across the cell cycle phases, which serves as a reference for evaluating the effects of EELD treatment. Administration of EELD at 1/5 IC_{50} resulted in a notable alteration in the cell cycle, with significant cell accumulation in the Sub G1 phase compared to the control group, which were 17.40 ± 0.10% and 10.40 ± 0.20%, respectively ($p<0.001$). This suggests that even at a lower concentration, EELD exerts measurable effects on cell cycle progression, likely through partial disruption

of regulatory checkpoints.Treatment with 1/2 IC_{50} of EELD demonstrated a more pronounced effect, with highly significant differences (**p<0.01 and ***p<0.001) in cell distribution across the phases. This concentration appears to strongly inhibit cell cycle progression, possibly inducing arrest at a Sub G1 phase compared to the control cells, which are 24.36 ± 0.30% and 10.40 ± 0.20%, respectively (p<0.001). Such an arrest could disrupt normal cell division and proliferation, contributing to EELD's cytotoxic activity against 4T1 cells.The dose-dependent response observed in this study underscores the potential mechanism of EELD as a cell cycle inhibitor, targeting specific checkpoints to hinder cancer cell proliferation. These findings suggest that EELD's anticancer effects may, in part, be mediated through modulation of the cell cycle, making it a promising candidate for further investigation in cancer therapy.

3.4. Apoptosis induces activity of EELD

The study observed the effect of EELD on the apoptosis induction of 4T1 cells. The analysis of apoptotic cells was investigated after the administration of EELD at 1/5 and 1/2 of its IC_{50} concentration. This activity was recorded after comparing with control cells, and it is presented in Figure 3.

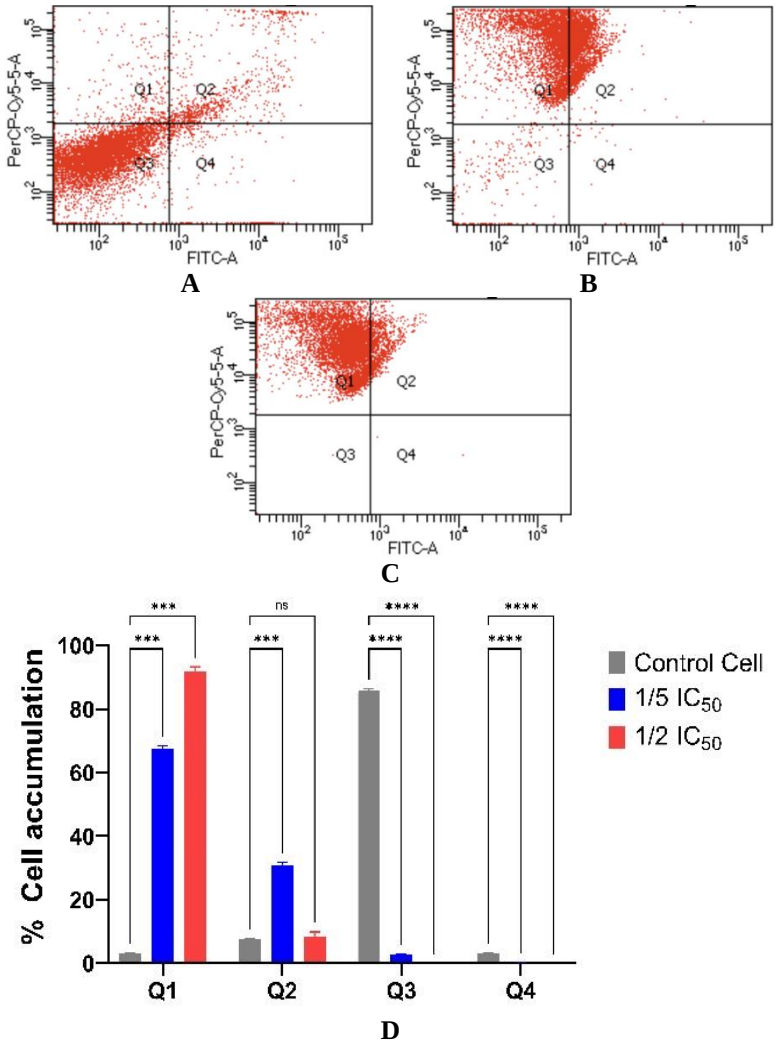

Figure (3): % Cell accumulation of 4T1 cells after administration of 1/5 and 1/2 IC_{50} of EELD. (A) The distribution of 4T1s cells in the control cell group, (B) 4T1 cells in 1/5 IC_{50} of the EELD group, (C) 4T1 cells in 1/2 IC_{50} of the EELD group, and (D) % Cell accumulation in each quadrant. Q1 indicated 4T1 cells going to necrosis, Q2 indicated 4T1 cells going to late apoptosis, Q3 indicated 4T1 cells going to live cells, and Q4 indicated going to early apoptosis. Meanwhile, *** indicates that the value is significantly different with p<0.0005, **** indicates that the value is significantly different with p<0.0001, and ^{ns} indicates that the value is not significantly different with p>0.05.

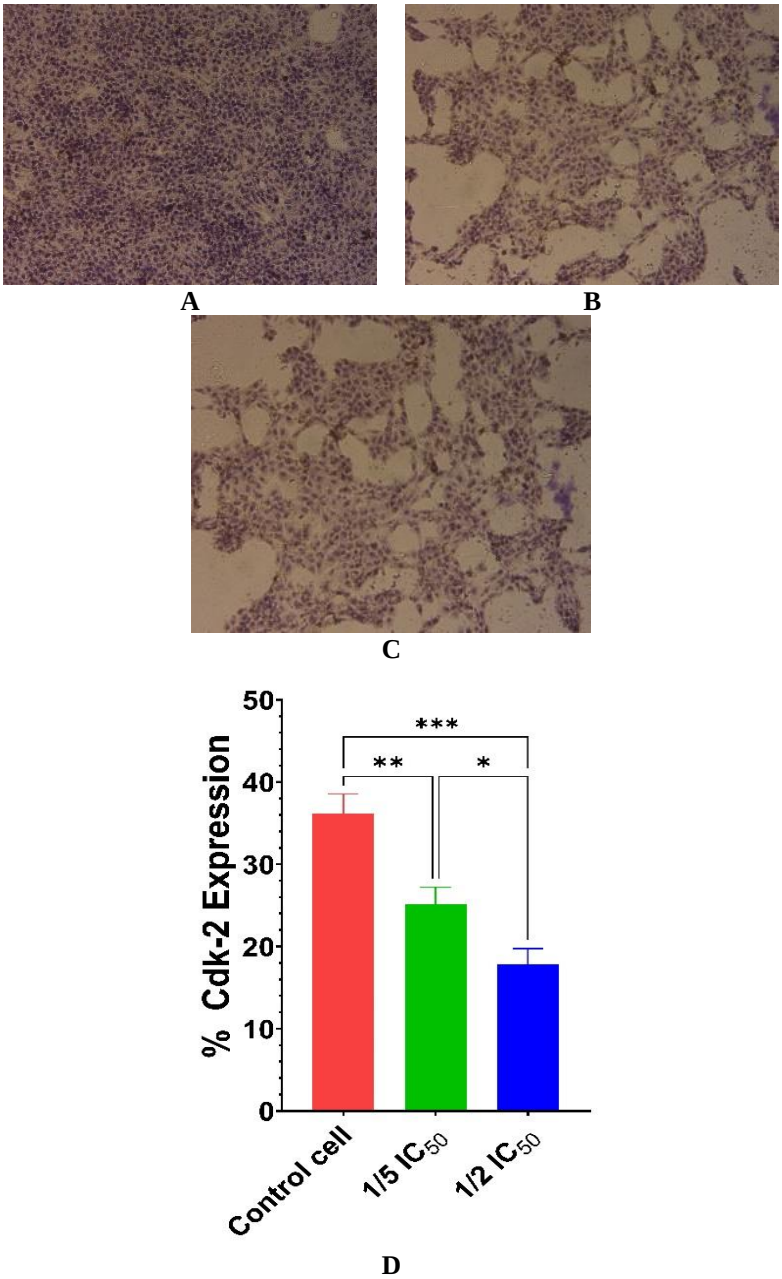

Figure (4): % Cdk-2 expression after administration of 1/5 and 1/2 IC_{50} of EELD. (A) Expression of Cdk-2 in the control cell group, (B) Expression of Cdk-2 in the 1/5 IC_{50} group, (C) Expression of Cdk-2 in the 1/2 IC_{50} group, and (D) The % expression of Cdk-2 in each group. Meanwhile, *indicates that the value is significantly different with $p<0.05$, **indicates that the value is significantly different with $p<0.01$, and *** indicates that the value is not significantly different with $p<0.001$.

Figure 3 evaluated the apoptosis-inducing activity of EELD on 4T1 cells, focusing on the distribution of cells in necrosis (Q1), late apoptosis (Q2), early apoptosis (Q4), and live cells (Q3). The data were analyzed after treating the cells with 1/5 and 1/2 of the IC_{50} concentrations of EELD. Statistical significance was assessed, with values denoted as ***$p<0.0005$, ****$p<0.0001$, and ns indicating non-significance ($p>0.05$).In the control group, the majority of cells were concentrated in the Q3 quadrant (live cells), reflecting normal viability and baseline apoptosis levels. Treatment with 1/5 IC50 of EELD significantly altered this distribution, with an increased

percentage of cells in Q4 (early apoptosis) and Q2 (late apoptosis), accompanied by a moderate rise in Q1 (necrotic cells), which are 0.313 ± 0.025%, 30.910 ± 0.737%, and 67.297 ± 1.173%, respectively. These results indicate that even at a lower concentration, EELD effectively initiates apoptotic pathways, leading to a shift from viability toward programmed cell death.At 1/2 IC_{50}, the effects of EELD were more pronounced, with a highly significant increase ($p<0.0001$) in Q2 and Q4 populations, which of 8.227 ± 1.613% and 0.00 ± 0.00%, respectively, compared to both the control and 1/5 IC_{50} groups. This indicates a robust induction of apoptosis, particularly in the late stage, suggesting that EELD's pro-apoptotic effects are concentration-dependent. The rise in Q1 (necrosis) remained moderate, further emphasizing apoptosis as the primary mechanism of cell death rather than necrosis.The dose-dependent induction of apoptosis by EELD demonstrates its potential as an effective anticancer agent targeting apoptotic pathways in 4T1 cells. These findings support the hypothesis that EELD disrupts critical survival signaling in cancer cells, promoting apoptotic processes that lead to cell death. Future investigations should aim to identify the molecular mechanisms underlying these effects, such as the involvement of intrinsic or extrinsic apoptotic pathways, to further validate EELD's therapeutic potential.

3.5. Cdk-2 and p-53 proteins expression

The immunocytochemistry (ICC) analysis of Cdk-2 protein expression in 4T1 cells under different conditions provides insight into its potential regulation and functional impact. The experimental conditions include control cells, cells treated with a 1/5 IC_{50} concentration of an EELD, and cells treated with a 1/2 IC_{50} concentration.The mean fluorescence intensity, indicative of Cdk-2 expression levels, decreases progressively across the conditions: 36.17 ± 2.38% in control cells, 25.16 ± 2.06% at 1/5 IC_{50}, and 17.86 ± 1.88% at 1/2 IC_{50} (Figure 4). Therefore, the statistical analysis of Cdk-2 expression levels in 4T1 cells across the three groups, including control cells, 1/5 IC_{50}, and 1/2 IC_{50}, revealed significant differences. A one-way ANOVA test showed a highly significant overall difference between the groups ($F = 37.30$, $p = 0.00041$). Post-hoc pairwise comparisons using Tukey's HSD test confirmed that all pairs of groups differ significantly from each other. Specifically, the control group exhibited significantly higher CDK-2 expression levels compared to both 1/5 IC_{50} and 1/2 IC_{50} ($p<0.05$). Similarly, the 1/5 IC_{50} group showed significantly higher expression than the 1/2 IC_{50} group ($p<0.05$). These findings indicate a dose-dependent suppression of Cdk-2 expression in response to the inhibitory agent. Such results underscore the efficacy of the treatment in modulating Cdk-2 expression and its potential implications for cell cycle regulation in 4T1 cells.Meanwhile, p53 protein expression in 4T1 cells treated with different concentrations of EELD (1/5 IC_{50} and 1/2 IC_{50}) demonstrates significant alterations in p53 expression compared to the control group (Figure 5). The data reveal a progressive increase in p53 expression as the concentration of EELD increases. Specifically, the mean percentage expression of p53 was 7.14 ± 1.17% in the control group, 19.90 ± 1.79% in the 1/5 IC_{50} group, and 29.52 ± 1.96% in the 1/2 IC_{50} group.

The statistical analysis of p53 expression levels in 4T1 cells treated with EELD (1/5 IC_{50} and 1/2 IC_{50}) and in the control group revealed significant differences among the groups. One-way ANOVA showed a highly significant overall difference ($F = 148.57$, $p < 0.0001$), indicating that p53 expression varies across the treatment conditions. Post-hoc pairwise comparisons using Tukey's HSD test confirmed that all group comparisons were statistically significant ($p < 0.05$). Specifically, the 1/5 IC_{50} group exhibited significantly higher p53 expression than the control group ($p<0.001$), while the 1/2 IC_{50} group showed even higher expression compared to both the control and 1/5 IC_{50} groups ($p<0.0001$ and $p<0.01$, respectively). These results confirm a dose-dependent upregulation of p53 expression with increasing concentrations of EELD, supporting its potential role in activating p53-mediated cellular responses, such as apoptosis, in 4T1 cells.

3.6. Phytochemical analysis of EELD using GC-MS

The GC-MS analysis of the EELD provides detailed information about the chemical composition of the fraction (Figure 6). The chromatogram reveals the presence of multiple compounds, identified by their retention times and relative abundances. Table 3 presents the major components, including hexadecanoic acid, methyl ester (19.16% of the total area), and trans-13-octadecenoic acid, methyl ester (20.24% of the total area), which are the most abundant compounds in the sample. These compounds are often associated with antioxidant and antimicrobial properties, highlighting the potential bioactivity of the EELD.

Other notable compounds include dodecanoic acid, methyl ester (7.04%), cis-13-octadecenoic acid (4.07%), and eicosane (4.18%), which contribute to the diverse chemical profile of the isolate. Trace components such as methyl tetradecanoate (2.84%) and isopropyl palmitate (0.64%) indicate the presence of methyl esters and fatty acid derivatives, which are known for their roles in biological systems as structural and signaling molecules. Additionally, the presence of ethyl iso-allocholate (0.27–1.36%) across several peaks suggests steroidal components that might contribute to anti-inflammatory or other pharmacological effects. The identified compounds and their relative abundances indicate a complex mixture, with potential applications in therapeutic or industrial contexts.

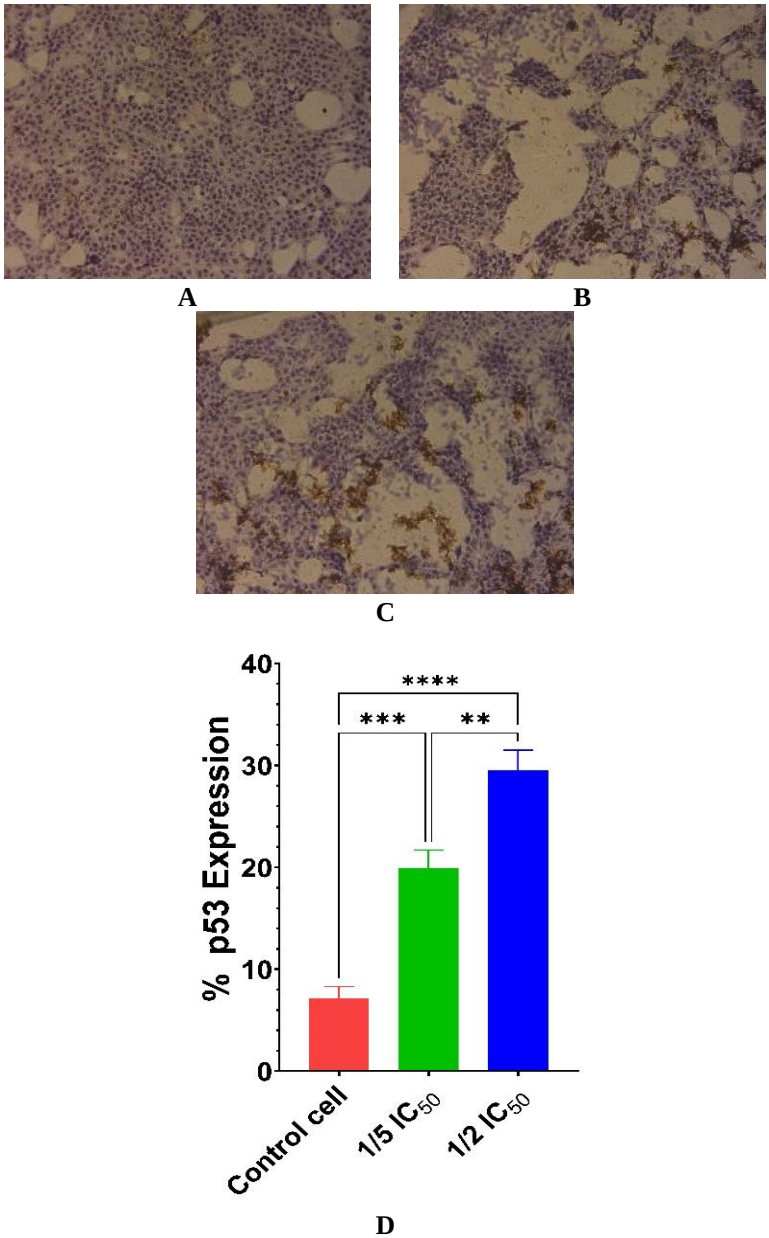

Figure (5): % p53 expression after administration of 1/5 and 1/2 IC_{50} of EELD. (A) Expression of p53 in the control cell group, (B) Expression of p53 in the 1/5 IC_{50} group, (C) Expression of p53 in the 1/2 IC_{50} group, and (D) The % expression of p53 in each group. Meanwhile, **indicates that the value is significantly different with $p<0.01$, *** indicates that the value is significantly different with $p<0.001$, and **** indicates that the value is not significantly different with $p<0.0001$.

4. Discussion

The findings of this study underscore the significant anticancer potential of the ethanolic extract and fractions derived from *L. domesticum* leaves, particularly the EELD fraction, against the murine 4T1 breast cancer cell line. The superior cytotoxic activity and selectivity of EELD, demonstrated by its low IC_{50} value and high selectivity index (SI), align with the growing body of evidence supporting the anticancer properties of plant-derived compounds [22], [23], [24]. However, its potency remains lower than that of doxorubicin, a standard chemotherapeutic agent, suggesting the need for further refinement and optimization [25].

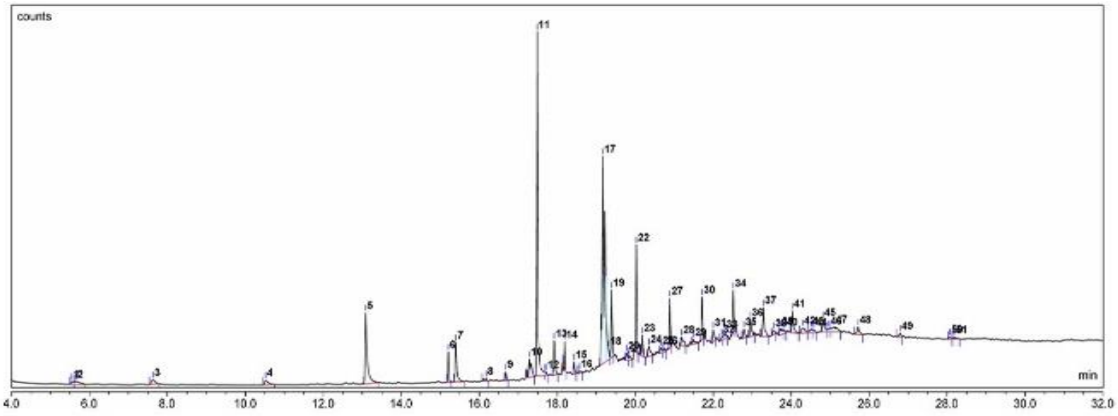

Figure (6): The GC-MS chromatogram of EELD

The mechanisms underlying EELD's anticancer activity appear to involve cell cycle arrest and apoptosis. Flow cytometry data revealed a dose-dependent arrest at the Sub G1 phase, indicative of DNA fragmentation, a hallmark of apoptosis [26], [27], [28]. This finding is consistent with studies showing that bioactive compounds from plant sources frequently target regulatory checkpoints in the cell cycle, thereby inhibiting proliferation and inducing cancer cell death [29], [30], [31]. Specifically, the ability of EELD to interfere with cell cycle progression suggests it may modulate key cell cycle regulators, such as cyclins and cyclin-dependent kinases (CDKs), which play crucial roles in maintaining cellular homeostasis and proliferation [32], [33], [34].

The induction of apoptosis by EELD was further corroborated through Annexin V-FITC/PI staining, which revealed a significant shift from live cells to apoptotic states in a dose-dependent manner. This observation is supported by the upregulation of p53 and downregulation of Cdk-2, as revealed by immunocytochemical analysis. The tumor suppressor protein p53, often termed the "guardian of the genome," orchestrates apoptosis by transactivating pro-apoptotic genes and downregulating anti-apoptotic proteins [35], [36], [37]. The suppression of Cdk-2 further supports this mechanism, as deregulated CDK activity is a hallmark of cancer progression and a common target for anticancer therapies [38], [39].

Phytochemical analysis of EELD identified the presence of bioactive compounds such as hexadecanoic acid, methyl ester, and trans-13-octadecenoic acid, methyl ester. These compounds are known for their antioxidant and anti-inflammatory properties, which may indirectly contribute to their anticancer effects [40], [41], [42]. For instance, oxidative stress and chronic inflammation are closely linked to carcinogenesis, and the antioxidant properties of these metabolites could mitigate such processes, enhancing their therapeutic efficacy [43]. Furthermore, fatty acid derivatives have been reported to influence cell membrane fluidity and signaling pathways, potentially disrupting cancer cell survival mechanisms [44], [45], [46].

These findings align with prior research demonstrating the anticancer properties of *L. domesticum*. Extracts of this plant have been reported to induce cell cycle arrest and apoptosis in various cancer cell lines, including colorectal and lung cancers, through modulation of pathways such as PI3K/Akt [12]. The bioactivity observed in EELD likely stems from a synergistic interaction of its constituents, emphasizing the importance of further fractionation and isolation to identify the most potent individual compounds.While these results are promising, they highlight the need for additional research. This study's in vitro nature requires validation through in vivo models to assess EELD's pharmacokinetics, bioavailability, and safety. Moreover, the precise molecular pathways involved in its anticancer effects, whether intrinsic or extrinsic apoptotic pathways, require further elucidation. Such insights will be crucial for developing EELD into a targeted anticancer therapy.

Table (3): The secondary metabolite compounds containing in EELD

RT (min)	Compound	Chemical formula	% Area
5.55	7-Methyl-Z-tetradecen-1-ol acetate	$C_{17}H_{32}O_2$	0.33
5.65	Hexadecane, 1,1-bis(dodecyloxy)-	$C_{40}H_{82}O_2$	0.83
7.63	Octanoicacid,methylester	$C_9H_{18}O_2$	0.84
10.52	Methyl8-methyl-nonanoate	$C_{11}H_{22}O_2$	0.83
13.08	Dodecanoicacid,methylester	$C_{13}H_{26}O_2$	7.04
15.20	Decane,5,6-bis(2,2-dimethylpropylidene)-,(E,Z)-	$C_{20}H_{38}$	1.37
15.40	Methyltetradecanoat	$C_{15}H_{30}O_2$	2.84
16.18	7-Methyl-Z-tetradecen-1-ol acetate	$C_{17}H_{32}O_2$	0.34
16.68	2-Pentadecanone, 6,10,14-trimethyl-	$C_{18}H_{36}O$	0.47
17.29	(Z)-Methylhexadec-11-enoate	$C_{17}H_{32}O_2$	1.99
17.49	Hexadecanoicacid,methylester	$C_{17}H_{34}O_2$	19.16
17.71	Cyclopropanebutanoicacid,2-[[2-[[2-[(2-pentylcyclopropyl	$C_{25}H_{42}O_2$	0.32
17.92	Dibutylphthalate	$C_{16}H_{22}O_4$	2.13
18.19	Eicosane	$C_{20}H_{42}$	0.73
18.43	Isopropylpalmitate	$C_{19}H_{38}O_2$	0.64
18.57	Ethyliso-allocholate	$C_{26}H_{44}O_5$	0.27
19.17	trans-13-Octadecenoicacid,methylester	$C_{19}H_{36}O_2$	20.24
19.39	Heptadecanoic acid, 16-methyl-, methyl ester	$C_{19}H_{38}O_2$	3.46
19.78	17-Pentatriacontene	$C_{35}H_{70}$	0.44
20.03	Eicosane	$C_{20}H_{42}$	4.18
20.18	cis-10-Nonadecenoicacid	$C_{19}H_{36}O_2$	1.18
20.89	Tetradecane,2,6,10-trimethyl-	$C_{17}H_{36}$	2.18
21.72	Tetrapentacontane,1,54-dibromo-	$C_{54}H_{108}Br_2$	2.05

5. Conclusions

In this study, the fraction EELD derived from *L. domesticum* leaves exhibited the most potent anticancer activity against 4T1 breast cancer cells among all tested fractions. The treatment induced Sub G1 cell cycle arrest and significantly increased apoptotic cell populations, accompanied by upregulation of the tumor suppressor protein p53 and downregulation of the cell cycle regulator CDK-2. These findings suggest that EELD triggers apoptosis through modulation of intrinsic pathways related to cell cycle arrest and apoptosis signaling. Given its selective cytotoxicity and mechanistic potential, EELD represents a promising candidate for further investigation as a plant-derived therapeutic agent against triple-negative breast cancer. Future research should explore *in vivo* efficacy, pharmacokinetics, and safety profiles to support its development into a potential anticancer formulation.

6. Conflicts of interest

There are no conflicts to declare

7. Acknowledgments

This work was supported by Universitas Sumatera Utara (Grant No. 27/UN5.2.3.1/PPM/KP-TALENTA/R/2023).

9. References

[1] M. Antonini *et al.*, “Male and female disparities in breast cancer epidemiology: A comparative cross-sectional analysis of a Brazilian cohort (2017–2021),” *Heliyon*, vol. 10, no. 18, p. e38183, Sep. 2024, doi: 10.1016/J.HELIYON.2024.E38183.

[2] E. Habibi *et al.*, “Alkaloid-rich extract of jujube seed regenerate the antiproliferative effect of paclitaxel on paclitaxel-resistant MDA-MB-231 breast cancer cell line in 2D and 3D cultures,” *J Agric Food Res*, vol. 18, p. 101438, Dec. 2024, doi: 10.1016/J.JAFR.2024.101438.

[3] C. S. Dzah and C. Agbemelo-Tsomafo, “Pro-oxidant Tetrapleuratetraptera polyphenol extract parallels quercetin as an in vitro cytotoxic agent in human liver cancer cells,” *Food and Humanity*, vol. 3, p. 100458, Dec. 2024, doi: 10.1016/J.FOOHUM.2024.100458.

[4] F. Yildiz, H. EcirogluSarban, F. G. Kocanci, M. Gungor, E. Yucel, and D. Yucel, “Phytochemical examination of Cistuslaurifolius extract and its impact on cytotoxicity, apoptosis and oxidative stress in colorectal and breast cancer cell lines,” *J Herb Med*, vol. 48, p. 100966, Dec. 2024, doi: 10.1016/J.HERMED.2024.100966.

[5] R. Arshad *et al.*, “Effects of pretreatment and drying temperatures on physicochemical and antioxidant properties of dried duku (Lansiumdomesticum),” *Measurement: Food*, vol. 14, p. 100148, Jun. 2024, doi: 10.1016/J.MEAFOO.2024.100148.

[6] K. L. Ji, M. Y. Dai, C. F. Xiao, and Y. K. Xu, “Two new steroids with NO inhibitory effects from lansiumdomesticum,” *Nat Prod Res*, vol. 35, no. 7, pp. 1147–1152, 2021, doi: 10.1080/14786419.2019.1643862.

[7] H. Febriani*et al.*, "Optimization of microwave-assisted extraction to obtain a polyphenol-rich crude extract from duku (Lansiumdomesticum Corr.) leaf and the correlation with antioxidant and cytotoxic activities," *Kuwait Journal of Science*, vol. 52, no. 1, p. 100315, Jan. 2025, doi: 10.1016/J.KJS.2024.100315.
[8] R. M. A. Khalili *et al.*, "Cytotoxicity effect and morphological study of different duku(Lansiumdomesticum corr.) Extract towards human colorectal adenocarcinoma cells line (HT-29)," *Pharmacognosy Journal*, vol. 9, no. 6, pp. 757–761, 2014, doi: 10.5530/pj.2017.6.119.
[9] A. Hardianto, S. S. Mardetia, W. Destiarani, Y. P. Budiman, D. Kurnia, and T. Mayanti, "Unveiling the Anti-Cancer Potential of OnoceranoidTriterpenes from Lansiumdomesticum Corr. cv. kokosan: An In Silico Study against Estrogen Receptor Alpha," *Int J Mol Sci*, vol. 24, no. 19, Oct. 2023, doi: 10.3390/ijms241915033.
[10] T. Mayanti*et al.*, "Toxicity evaluation of ethanol extract of lansiumdomesticum cv kokossan seeds in female wistar rats," *Tropical Journal of Natural Product Research*, vol. 4, no. 8, pp. 348–354, 2020, doi: 10.26538/tjnpr/v4i8.5.
[11] S. Purwani, J. Nahar, Z. Zulfikar, N. Nurlelasari, and T. Mayanti, "Molecular Docking on Kokosanolide A and C for Anticancer Activity Against Human Breast Cancer Cell MCF-7," *Jurnal Kimia Valensi*, vol. 7, no. 1, pp. 52–57, 2021, doi: 10.15408/jkv.v7i1.20534.
[12] M. F. Lubis, P. A. Z. Hasibuan, H. Syahputra, J. M. Keliat, V. E. Kaban, and R. Astyka, "Duku (Lansiumdomesticum) Leaves Extract Induces Cell Cycle Arrest and Apoptosis of HepG2 Cells via PI3K/Akt Pathways," *Trends in Sciences*, vol. 20, no. 2, Feb. 2023, doi: 10.48048/tis.2023.6437.
[13] T. Mayanti*et al.*, "OnoceranoidTriterpenes of Lansiumdomesticum Corr. cv. Kokossan and Their Cytotoxicity against MCF-7 Breast Cancer Cells," *Trends in Sciences*, vol. 22, no. 1, Jan. 2024, doi: 10.48048/tis.2025.9000.
[14] K. Fadhilah, S. Wahyuono, and P. Astuti, "Fractions and isolated compounds from lansiumdomesticum fruit peel exhibited cytotoxic activity against t-47d and hepg2 cell lines," *Biodiversitas*, vol. 22, pp. 3743–3748, 2021, doi: 10.13057/biodiv/d220918.
[15] H. Febriani*et al.*, "Optimization of microwave-assisted extraction to obtain a polyphenol-rich crude extract from duku (Lansiumdomesticum Corr.) leaf and the correlation with antioxidant and cytotoxic activities," *Kuwait Journal of Science*, vol. 52, no. 1, p. 100315, Jan. 2025, doi: 10.1016/J.KJS.2024.100315.
[16] M. F. Lubis *et al.*, "Cytotoxic activity of the purified extracts from duku (Lansiumdomesticum Corr.) Leaf against MCF-7 and HTB-183 cell lines, and the correlation with antioxidant activity," *Journal of Medicinal and Pharmaceutical Chemistry Research*, vol. 5, no. 12, pp. 1159–1172, Dec. 2023, doi: 10.48309/jmpcr.2023.182193.
[17] K. Fitri *et al.*, "SYNTHESIS OF SILVER NANOPARTICLES USING ETHANOLIC EXTRACT OF NelumbonuciferaGaertn . LEAF AND ITS CYTOTOXIC ACTIVITY AGAINST T47D AND 4T1 CELL LINES," *Rasayan Journal of Chemistry*, vol. 16, no. 1, pp. 104–110, 2023.
[18] P. A. Z. Hasibuan, J. M. Keliat, and M. F. Lubis, "Combination of cisplatin and ethyl acetate extract of Vernonia amygdalina Delile induces cell cycle arrest and apoptosis on PANC-1 cells via PI3K/mTOR," *J Pharm Pharmacogn Res*, vol. 12, no. 5, pp. 870–880, Sep. 2024, doi: 10.56499/jppres23.1748_12.5.870.
[19] M. F. Lubis, S. Sumaiyah, L. D. Lubis, K. Fitri, and R. Astyka, "Application of Box-Behnken design for optimization of Vernonia amygdalina stem bark extract in relation to its antioxidant and anti-colon cancer activity," *Arabian Journal of Chemistry*, vol. 17, no. 4, p. 105702, Apr. 2024, doi: 10.1016/J.ARABJC.2024.105702.
[20] P. A. Z. Hasibuan, U. Harahap, P. Sitorus, and D. Satria, "The anticancer activities of Vernonia amygdalina Delile. Leaves on 4T1 breast cancer cells through phosphoinositide 3-kinase (PI3K) pathway," *Heliyon*, vol. 6, no. 7, p. e04449, 2020, doi: 10.1016/j.heliyon.2020.e04449.
[21] K. Fitri, M. F. Lubis, H. Syahputra, R. Astyka, and V. E. Kaban, "PHYTOCHEMICALS ANALYSIS OF Baccaureamotleyana Mull. Arg. EXTRACTS AND ANTIPROLIFERATION EFFECT AGAINST PANC-1 CELL THROUGH p53 AND Bcl-2 EXPRESSIONS," *Rasayan Journal of Chemistry*, vol. 16, no. 3, pp. 1516–1524, Jul. 2023, doi: 10.31788/RJC.2023.1638326.
[22] R. Al-Nemari *et al.*, "Cytotoxic effects of Annona squamosa leaves against breast cancer cells via apoptotic signaling proteins," *J King Saud UnivSci*, vol. 34, no. 4, p. 102013, Jun. 2022, doi: 10.1016/J.JKSUS.2022.102013.
[23] H. R. Mohamed, E. A. El-Wakil, M. M. Hamed, and Z. A. E. K. El-Shahid, "Phytochemical Profiling, Cytotoxicity and Anti-inflammatory Potential of Salvia hispanica L. Seeds," *Egypt J Chem*, vol. 67, no. 12, pp. 409–422, Dec. 2024, doi: 10.21608/ejchem.2024.303803.10000.
[24] A. Beltagy, hend Al-koriety, G. Omran, and H. Zaatout, "In-vitro Promising Anticancer activity of Murrayapaniculata L. Leaves extract against three cell lines and isolation of two new major compounds from the extract," *Egypt J Chem*, vol. 0, no. 0, pp. 0–0, May 2024, doi: 10.21608/ejchem.2024.266841.9268.
[25] G. Jargalsaikhan, J. Y. Wu, Y. C. Chen, L. L. Yang, and M. S. Wu, "Comparison of the phytochemical properties, antioxidant activity and cytotoxic effect on HepG2 cells in mongolian and taiwanese rhubarb species," *Molecules*, vol. 26, no. 5, 2021, doi: 10.3390/molecules26051217.
[26] R. Kanlaya, C. Subkod, S. Nanthawuttiphan, and V. Thongboonkerd, "Caffeine causes cell cycle arrest at G0/G1 and increases of ubiquitinated proteins, ATP and mitochondrial membrane potential in renal cells," *ComputStructBiotechnol J*, vol. 21, pp. 4552–4566, Jan. 2023, doi: 10.1016/J.CSBJ.2023.09.023.
[27] M. Kwon *et al.*, "Kurarinone induced p53-independent G0/G1 cell cycle arrest by degradation of K-RAS via WDR76 in human colorectal cancer cells," *Eur J Pharmacol*, vol. 923, p. 174938, May 2022, doi: 10.1016/J.EJPHAR.2022.174938.
[28] S. M. Abdelnasser and N. Abu-Shahba, "Bacillus sonorinses derived exopolysaccharide enhances cell cycle arrest, apoptosis, necrosis, autophagy and COX-2 down regulation in liver cancer cells," *Biotechnology Reports*, vol. 43, p. e00848, Sep. 2024, doi: 10.1016/J.BTRE.2024.E00848.

[29] M. S. Bastos *et al.*, "Moquiniastrumpolymorphum subsp. polymorphum extract inhibits the proliferation of an activated hepatic stellate cell line (GRX) by regulating the p27 pathway to generate cell cycle arrest," *J Ethnopharmacol*, vol. 303, p. 116056, Mar. 2023, doi: 10.1016/J.JEP.2022.116056.

[30] V. M. A. S. Grinevicius, K. S. Andrade, F. Ourique, G. A. Micke, S. R. S. Ferreira, and R. C. Pedrosa, "Antitumor activity of conventional and supercritical extracts from Piper nigrum L. cultivar Bragantina through cell cycle arrest and apoptosis induction," *J Supercrit Fluids*, vol. 128, pp. 94–101, Oct. 2017, doi: 10.1016/J.SUPFLU.2017.05.009.

[31] F. Abo-Elghiet, M. H. Ibrahim, M. A. El Hassab, A. Bader, Q. M. A. Abdallah, and A. Temraz, "LC/MS analysis of ViscumcruciatumSieber ex Boiss. extract with anti-proliferative activity against MCF-7 cell line via G0/G1 cell cycle arrest: An in-silico and in-vitro study," *J Ethnopharmacol*, vol. 295, p. 115439, Sep. 2022, doi: 10.1016/J.JEP.2022.115439.

[32] H. Kim *et al.*, "Krill oil ameliorates benign prostatic hyperplasia by regulating G1-phase cell cycle arrest and altering signaling pathways and benign prostatic hyperplasia-associated markers," *Food Science and Human Wellness*, vol. 13, no. 6, pp. 3311–3324, Nov. 2024, doi: 10.26599/FSHW.2023.9250017.

[33] A. A. Kashmiry, N. S. Ibrahim, M. F. Mohamed, and I. A. Abdelhamid, "Novel α-Cyano-Indolyl Chalcones as Anti-Cancer Candidates, Induce G1/S Cell Cycle Arrest and Sequentially Activate Caspases-7, 8, and 9 in Breast Carcinoma," *PolycyclAromatCompd*, Oct. 2024, doi: 10.1080/10406638.2024.2412818.

[34] M. Abohendia, A. M. Metwally, W. Hozayen, A. O. El-Gendy, and A. H. A. Abdel Wahab, "Decitabine attenuates the anti-cancer effect of doxorubicin by repressing ECDH1 and inducing SNAI1 and BCL2 in HepG2 hepatocellular carcinoma cells.," *Egypt J Chem*, vol. 66, no. 13, pp. 745–754, Dec. 2023, doi: 10.21608/EJCHEM.2023.181289.7341.

[35] Y. Hirose, S. Sato, K. Hashiya, M. Ooga, T. Bando, and H. Sugiyama, "Chb-M′, an Inhibitor of the RUNX Family Binding to DNA, Induces Apoptosis in p53-Mutated Non-Small Cell Lung Cancer and Inhibits Tumor Growth and Repopulation In Vivo," *J Med Chem*, vol. 67, no. 11, pp. 9165–9172, Jun. 2024, doi: 10.1021/ACS.JMEDCHEM.4C00315.

[36] M. G. F. Guefack*et al.*, "Hypericumroeperianum bark extract suppresses breast cancer proliferation via induction of apoptosis, downregulation of PI3K/Akt/mTORsignaling cascade and reversal of EMT," *J Ethnopharmacol*, vol. 319, p. 117093, Jan. 2024, doi: 10.1016/J.JEP.2023.117093.

[37] J. Liu *et al.*, "Green formulation of iron nanoparticles by plant extract induces apoptosis via P53 and STAT3 signaling pathways in prostate cancer cells," *Inorg Chem Commun*, vol. 162, p. 112164, Apr. 2024, doi: 10.1016/J.INOCHE.2024.112164.

[38] T. Roy *et al.*, "Synthesis, inverse docking-assisted identification and in vitro biological characterization of Flavonol-based analogs of fisetin as c-Kit, CDK2 and mTOR inhibitors against melanoma and non-melanoma skin cancers," *BioorgChem*, vol. 107, p. 104595, Feb. 2021, doi: 10.1016/J.BIOORG.2020.104595.

[39] O. A. Hamed, N. Abou-Elmagd El-Sayed, W. R. Mahmoud, and G. F. Elmasry, "Molecular docking approach for the design and synthesis of new pyrazolopyrimidineanalogs of roscovitine as potential CDK2 inhibitors endowed with pronounced anticancer activity," *BioorgChem*, vol. 147, p. 107413, Jun. 2024, doi: 10.1016/J.BIOORG.2024.107413.

[40] M. E. Effiong, M. Bella-Omunagbe, I. S. Afolabi, and S. N. Chinedu, "In silico evaluation of potential breast cancer receptor antagonists from GC-MS and HPLC identified compounds in Pleurotus ostreatus extracts," *RSC Adv*, vol. 14, no. 33, pp. 23744–23771, Jul. 2024, doi: 10.1039/D4RA03832K.

[41] I. A. Al-Hakami, A. El-Shaibany, H. Al-Mahbashi, A. S. Abdelkhalek, M. M. Elaasser, and A. E. Raslan, "GC-MS profiling and evaluation of acute oral toxicity, anti-tumour, antimicrobial and antioxidant activities of Croton socotranusBalf.f. aerial parts: in-vitro, in-vivo and in-silico studies," *Nat Prod Res*, vol. 38, no. 24, pp. 4307–4316, Dec. 2024, doi: 10.1080/14786419.2023.2280820.

[42] M. F. Khan, R. F. Alanazi, A. A. Baabbad, N. D. Almoutiri, and M. A. Wadaan, "Angiogenic protein profiling, phytochemical screening and in silico anti-cancer targets validation of stem, leaves, fruit, and seeds of Calotropisprocera in human liver and breast cancer cell lines," *Environ Res*, vol. 256, p. 119180, Sep. 2024, doi: 10.1016/J.ENVRES.2024.119180.

[43] G. A. Moriasi, A. M. Ireri, E. M. Nelson, and M. P. Ngugi, "In vivo anti-inflammatory, anti-nociceptive, and in vitro antioxidant efficacy, and acute oral toxicity effects of the aqueous and methanolic stem bark extracts of Lonchocarpuseriocalyx (Harms.)," *Heliyon*, vol. 7, no. 5, p. e07145, May 2021, doi: 10.1016/J.HELIYON.2021.E07145.

[44] C. A. Ukwubile, A. Ahmed, U. A. Katsayal, J. Ya'u, and H. Nettey, "Chitosan nanoparticle-mediated drug delivery for linoleic acid isolated from Melastomastrumcapitatum Fern. leaf extract against MCF-7 and OV7 cancer cells," *Pharmacological Research - Natural Products*, vol. 5, p. 100105, Dec. 2024, doi: 10.1016/J.PRENAP.2024.100105.

[45] A. Hu *et al.*, "A novel CPT1A covalent inhibitor modulates fatty acid oxidation and CPT1A-VDAC1 axis with therapeutic potential for colorectal cancer," *Redox Biol*, vol. 68, p. 102959, Dec. 2023, doi: 10.1016/J.REDOX.2023.102959.

[46] N. Askari and S. M. Mansouri, "Fatty acid composition and anti-cancer activity of essential oil from Tenebriomolitor larvae in combination with zoledronic acid on prostate cancer," *Heliyon*, vol. 10, no. 21, p. e40012, Nov. 2024, doi: 10.1016/J.HELIYON.2024.E40012.